

© 2019. This is the pre-print (submitted) version of the following article: “K. Wagner, G. Häggström, N. Skoglund, J. Priscak, M. Kuba, M. Öhman, H. Hofbauer, Layer formation mechanism of K-feldspar in bubbling fluidized bed combustion of phosphorus-lean and phosphorus-rich residual biomass, Applied Energy. 248 (2019) 545–554. <https://doi.org/10.1016/j.apenergy.2019.04.112>.”, which has been published in final form at <https://doi.org/10.1016/j.apenergy.2019.04.112>. This pre-print version is made available under the CC-BY-NC-ND 4.0 license <http://creativecommons.org/licenses/by-nc-nd/4.0/>.

Layer Formation Mechanism of K-feldspar in Bubbling Fluidized Bed Combustion of Phosphorus-lean and Phosphorus-rich Residual Biomass

Katharina Wagner^{1,2,*}, Gustav Häggström³, Nils Skoglund^{1,2,4}, Juraj Priscak^{1,2}, Matthias Kuba^{1,2,3,4,*}, Marcus Öhman³, Hermann Hofbauer²

¹ Bioenergy 2020+ GmbH, Wienerstraße 49, A-7540 Güssing, Austria

² Institute of Chemical, Environmental & Bioscience Engineering, Technische Universität Wien, Getreidemarkt 9/166, A-1060 Vienna, Austria

³ Energy Engineering, Division of Energy Science, Luleå University of Technology, SE-971 87 Luleå, Sweden

⁴ Thermochemical Energy Conversion Laboratory, Umeå University, SE-901 87 Umeå, Sweden

*Corresponding author: matthias.kuba@bioenergy2020.eu

katharina.wagner@bioenergy2020.eu

Abstract

The use of phosphorus-rich fuels in fluidized bed combustion is one probable way to support both heat and power production and phosphorus recovery. Ash is accumulating in the bed during combustion and interacting with the bed material to form layers and/or agglomerates possibly removing phosphorus from the bed ash fraction. To further deepen the knowledge about the differences in mechanisms behind the ash chemistry of phosphorus-lean and phosphorus-rich fuels, experiments in a 5 kW bench-scale-fluidized bed test-rig with K-feldspar as bed material were conducted with bark, wheat straw, chicken manure, and chicken manure admixtures to bark and straw. Bed material samples were collected and studied for layer formation and agglomeration phenomena. It was observed that the admixture of phosphorus-rich chicken manure to bark changed the layer formation mechanism, shifting the chemistry to the formation of phosphates rather than silicates. The admixture of chicken manure to straw reduced the ash melting and agglomeration risk, making it possible to increase the time until defluidisation of the fluidized bed occurred. The results also highlight that an increased ash content does not necessarily lead to more ash melting related problems as long as the ash melting temperature is high enough.

Keywords: phosphorus, layer formation, agglomeration, K-feldspar, fluidized bed

Highlights

- Phosphorus-rich fuels shift the ash chemistry to the formation of phosphates
- The admixture of chicken manure to straw increases the time until defluidisation
- The fuel ash content is not a fitting parameter to predict bed defluidisation
- K-feldspar is less susceptible to layer formation compared to quartz

Introduction

Biomass is a non-fluctuating available renewable energy source and also the only renewable carbon source, well suited for the production of carbon-based goods, such as fuels or chemicals. The most widely used biomass in energy conversion processes is forest-derived but increasing demand increases its stock prices [1,2] and leads to the necessity to research alternative bio-based fuels. Logging residues are cheaper wood-based alternatives [3], which could be able to substitute parts or the entire logging wood used in biomass-fueled plants for heat and power production. Agricultural waste is a source of biomass that increasingly gains attention, as well as waste streams like sewage sludge and municipal waste, which behave differently to woody-based biomass and therefore need more caution when used in thermochemical energy conversion processes.

An important challenge in switching from woody-type fuels to other biomass in energy applications is the ash forming elements in such alternative biomass fuels. For combustion and gasification applications, fluidized beds are especially suitable when more challenging, alternative fuels are used, since fluidized beds are rather flexible regarding the used fuel [4]. Advantages of a fluidized bed are the rapid mixing of particles, ensuring nearly isothermal conditions in the bed, its suitability for large scale processes, and an increased heat transfer between bed material and fluid [5].

Several studies have shown an interaction between the bed material used in fluidized beds and ash contained in fuel. This interaction can lead to agglomerations [4,6–8], deposits [3,9] and layer formation [10–15] on bed material particles. The different mechanisms dominating the particle layer formation on quartz were summarized by Brus et al. [8]. Mechanism (a) describes a bed layer formation initiated by a potassium silicate melt, which is followed by calcium diffusion. Mechanism (b) describes the direct reaction of potassium in gaseous phases with the bed particle, which leads to low melting silicate layers. Mechanism (c) describes the direct adhesion of partly molten ash-derived potassium silicate particles on bed particles. These mechanisms have been found to be suitable to describe the occurring phenomena [10,13,15] and were further developed for various biomass fuels [7,16].

Due to the observed problems of agglomeration and deposition formation with quartz beds [7,16,17], several alternative bed materials, like olivine [6], K-feldspar [6], magnesite [17–19], calcite [18,19], dolomite [17], sillimanite [18], bauxite [18], and plagioclase [6], were tested for their suitability in fluidized bed applications. Further studies on K-feldspar focused on the layer formation in combustion [14] and gasification atmosphere [12], or a direct comparison of both [20]. Berguerand and Berdugo Vilches tested Alkali-feldspar (a mixture of K- and Na-feldspar with impurities of Ca-feldspar) in the Chalmers 2 MW indirect gasifier as bed material for gasification applications with wood. During the experiment duration of 1 week a layer rich in calcium, potassium, magnesium, and sodium was formed [21]. An ash-rich fuel mixture was tested by Wagner et al. in a 100 kW dual fluidized bed steam gasifier at TU Wien with K-feldspar as bed material [22]. The observed layers were rich in calcium,

phosphorus, and magnesium and increased the catalytic activity of the bed material regarding gasification reactions (e.g. steam reforming and water-gas-shift reaction).

Phosphorus is a main ash forming element which influences the ash chemistry in thermochemical conversion processes when present in sufficient concentrations, which is not uncommon in agricultural waste streams. This phosphorus-rich ash results in increased phosphate formation rather than silicate-formation, which is occurring for woody-based fuel [23]. For a quartz bed, changes in ash chemistry based on phosphorus content could be observed in the gas phase [23] and through its influences on bed agglomeration tendencies [4]. Phosphorus-rich fuels were tested in a gasifier and in combustion atmosphere in combination with K-feldspar [20,22] also giving a first proposal regarding a possible layer forming mechanism on K-feldspar. Further, the importance of phosphorus as a nutrient is recognized among the planetary boundaries along with eight other criteria [24]. The introduction of agricultural waste streams may not only require changes to process conditions such as bed material choice, but also facilitate phosphorus recovery either by direct use of ash fractions or through phosphate recovery technologies [25–27].

The aim of this paper is therefore to give an insight in the differences in the interaction of K-feldspar bed material and ash forming elements in three different biomass fuels; bark, wheat straw, and chicken manure. Mixtures of chicken manure with bark and straw should highlight the influence of phosphorus on layer formation and agglomeration mechanisms. This work should simultaneously provide an insight in the behavior of K-feldspar as an alternative bed material and its suitability for the fluidized bed combustion of low ash-melting and phosphorus-rich fuels.

Materials and Methods

Residual fuels used in the experiments

The fuels used in these experiments were bark, wheat straw, and chicken manure as exemplary biomass residues for combustion in fluidized beds. Bark was chosen as a low-quality wood-based fuel and chicken manure as a phosphorous-rich fuel. Straw was selected as a typical agricultural biomass with high potassium and high silica content, expected to form low-temperature melting potassium silicates. Mixtures of bark and straw with chicken manure were used to study the influence of phosphorus on the ash melting and ash layer formation when the amount of phosphorus is increased in the ash. Apart from the pure fuels the following mixtures were studied: 90% bark + 10% chicken manure (B9:C1), 70% bark + 30% chicken manure (B7:C3), 90% straw + 10% chicken manure (S9:C1), and 70% straw + 30% chicken manure (S7:C3). The ratios were calculated based on dry masses and all fuels were prepared as 6 mm pellets. Some relevant ash related properties of these fuels are summarized in Table 1.

		Ash content	LHV ^b d.b. ^a	Deformation temperature
Fuels and mixtures	Abbreviation	Mass fraction given in % d.b. ^a	kJ kg ⁻¹	°C
Bark	B	8.1	18180	1160
Wheat straw	S	7.5	16860	830
Chicken manure	C	25.4	13900	>1490
Mixture of 90 % bark and	B9:C1	9.5	17500	1230

10% chicken manure				
Mixture of 70 % bark and 30% chicken manure	B7:C3	13.5	16430	>1490
Mixture of 90 % straw and 10% chicken manure	S9:C1	9.0	16900	880
Mixture of 70 % straw and 30% chicken manure	S7:C3	13.0	16010	1170

Table 1. Relevant properties of the used fuels.

^a dry basis; ^b lower heating value

The ash content was determined according to DIN 14775 but at a temperature of 550 °C, the lower heating value was determined according to DIN 51900 T2, and the ash deformation temperature was determined according to DIN 51730. The elemental composition of the ash was determined with X-ray fluorescence (Panalytical Axios with a Rh X-ray tube, 50 kV excitation voltage, tube current of 50 mA, measured under vacuum). Figure 1 shows the “fuel fingerprints” of the used fuels which displays the ash composition in mol kg⁻¹ instead of oxides, which facilitates a direct comparison of concentrations of ash forming elements aiming to enable determination of probable ash formation reactions. The exact concentration values are provided as supplementary information in Table S. 1.

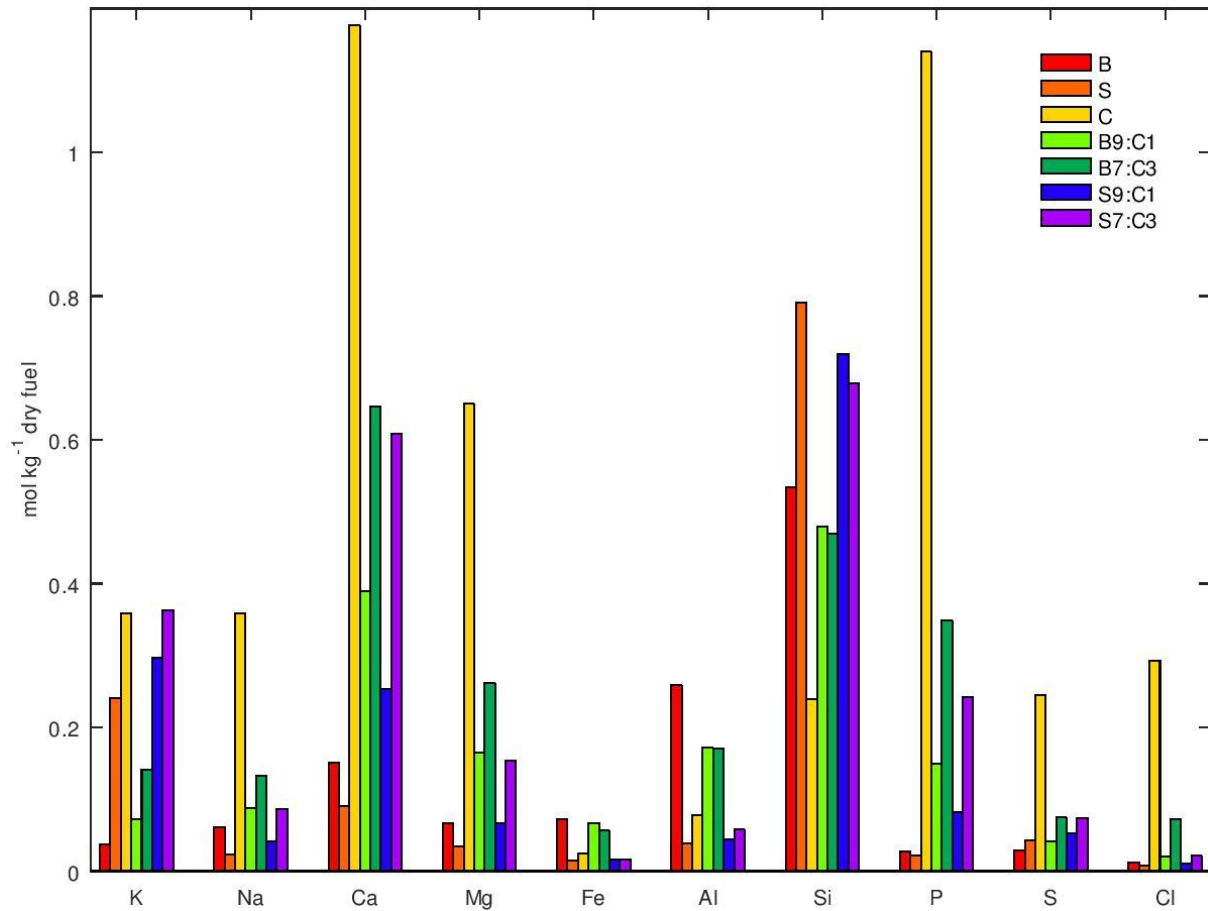


Figure 1. Composition of main ash forming elements shown as a fuel fingerprint for the fuels and fuel mixtures.

Bed material

K-feldspar was chosen as an alternative bed material to quartz in this study since it has already shown to be an interesting bed material since it is also able to develop layers [6,12,14,20–22]. Additionally, mechanical properties of K-feldspar relevant for fluidization are similar to the properties of quartz, as seen in Table 2, therefore ensuring similar fluid dynamic behavior in a fluidized bed.

	Quartz [28]	K-feldspar
mohs' hardness	7	6
density in kg·m ⁻³	2650	2600

Table 2. Mechanical properties of quartz and K-feldspar.

The received K-feldspar was sieved to a particle size range of 200 – 250 μm as needed for the bench-scale test-rig described below. The unsieved bed material contains 4 % quartz [29], due to the specific source, therefore, in later discussions of the results ash and bed material interactions will be addressed for K-feldspar and additionally for quartz as a benchmark bed material.

Bench-scale fluidized bed reactor

The experiments were conducted in a 5 kW bubbling fluidized bed, depicted in Figure 2. The total height of the fluidized bed is 2 m with an inner diameter of 100 mm of the fluidized bed and 200 mm in the freeboard section. An air flow of 50 NL/min was used as bottom air for the fluidized bed, and a secondary air flow of 30 NL/min was introduced above the fluidized bed into the freeboard to ensure complete combustion. The reactor is covered with heaters to ensure a more homogeneous temperature profile along the reactor height. The temperature

inside the reactor is regulated by these heaters as well as by the fuel input. Temperatures and differential pressure over the bed were monitored continuously. The flue gas is cleaned by a cyclone removing all particles bigger than 10 μm . Afterwards the flue gas is further cleaned in a water scrubber. A more detailed description of the reactor has been published by Öhman and Nordin [30].

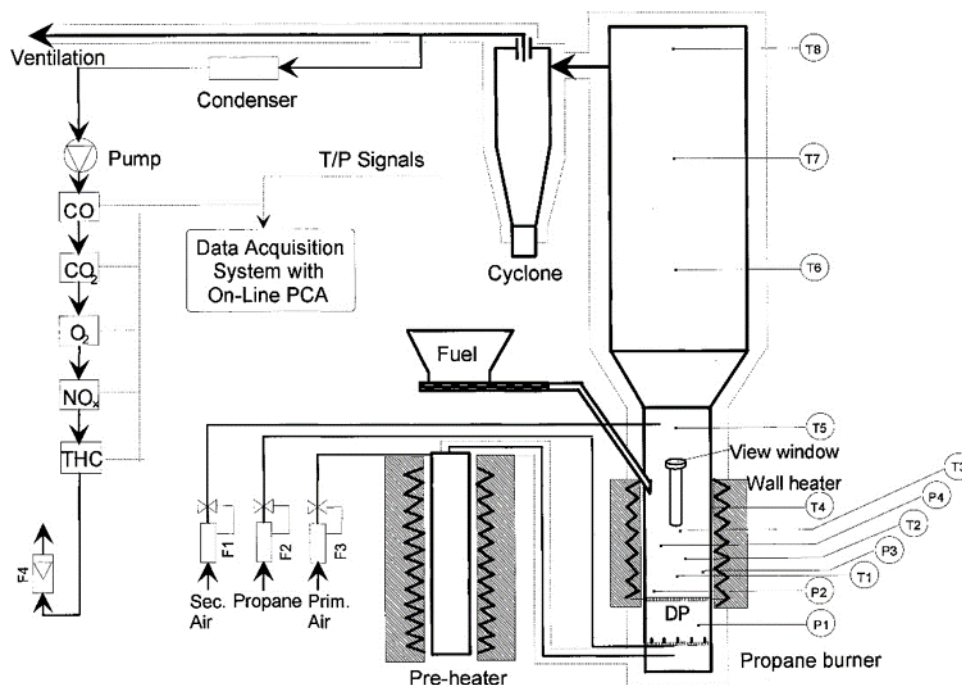


Figure 2. Schematic of the 5 kW bubbling fluidized bed reactor used for the combustion experiments. Reprinted with permission from [30]. Copyright 1998 American Chemical Society.

540 g of the sieved bed material were used for the investigations. The reactor was electrically heated up to the desired operating temperature, which ranged from 730 to 830 $^{\circ}\text{C}$, and then fuel feed was started. The operating temperature was chosen in the lower spectrum for straw and its blends since they are more prone to ash melting, while bark and its blends were operated at higher temperatures since the fuel ash has a higher deformation temperature (Table 1). Fuel was fed continuously with a rate around 0.7 kg h^{-1} for 40 hours or until the bed collapsed due to agglomeration. Bed material samples were taken at the end of each experiment after the reactor cooled down. To ensure a combustion atmosphere the flue gas composition was measured with an FTIR detector and it was ensured to keep the O_2 concentration above 6 %.

Morphological and elemental analysis

Collected bed samples were embedded in an epoxy-based resin. The epoxy disc was subsequently polished to obtain cross-sections of the bed particles, both ash and bed material, which could be used for determination of layer growth and composition. Elemental analysis of the layers on the bed material was carried out with a Carl Zeiss Evo LS15 scanning electron microscope (SEM) equipped with an Oxford X-Max 80 energy dispersive X-ray spectrometer (EDS). The measurements conducted were line scans over the layers and area analysis to obtain a distribution of elements. For each sample, 10 typical K-feldspar bed grains were chosen randomly and EDS line analysis was done across the layers on 3 evenly spaced locations on each grain. All layers obtained for a sample were studied for areas of constant concentration segments and the average was calculated for each of those segments. The clustering algorithm DBSCAN [31] grouped the segments according to similar

concentrations in the profile. The received groups were then named as an inner or outer layer, depending on the location on the particle.

Results and discussion

In the following section, results related to ash and bed material interaction gained from the experimental and analytic study will be presented and discussed. First, an overview of the experimental parameters and operating times of the single experiments will be addressed. This is followed by a presentation of the morphology and composition of the bed particle layers resulting from the interaction with fuel ash. Based on these results, the mechanism underlying the ash – bed material interaction will be assessed. Finally, an evaluation of the suitability of K-feldspar with different fuels and fuel mixtures will be conducted based on the findings from the layer formation and ash chemistry investigations.

Combustion characteristics of fuels and fuel mixtures

Table 3 provides a summary of all conducted experiments with the average bed temperature (calculated as the average of lower and upper bed temperature during stable operation), the time it took for the bed to defluidise, and the estimated amount of ash (based on the fuel ash content) fed to the system. Bed ash cannot be continually discharged from the reactor during experiments so the accumulation of bed ash did affect fluidization in some long-running experiments.

	Bed temperature	Defluidisation time	Total ash fed into the reactor
Fuels	°C	hours	g
B	826±8	36.52	1501
S	735±21	5.52	231
C	804±4	10.83	2039
B9:C1	798±3	-	2558
B7:C3	795±4	-	4027
S9:C1	753±11	5.48	287
S7:C3	790±10	9.55	828

Table 3. Combustion characteristics stated as average bed temperature, time until defluidisation occurred, and the total ash fed to the system during each experiment.

When pure bark was used as fuel, the bed defluidised after 36.5 hours due to such accumulation of bed ash. This was determined to be caused by the large amount of bed ash rather than interaction between ash-forming elements and bed material after investigation with SEM-EDS. In contrast to this, combustion of straw defluidised already after 5.5 h due to formation of agglomerates. The experiment with only chicken manure as fuel was stopped earlier than 40 hours due to the accumulation of bed ash. Only the two experiments with bark and chicken manure mixtures lasted for the planned 40 hours and no signs of agglomeration or other problems were observed. Thus, only mixtures of bark and chicken manure did not lead to agglomeration- or ash accumulation-based shut-downs. By co-combusting 70% straw with 30% chicken manure (0.13 mass fraction ash) it was possible to increase the operational time to nearly 10 h at a higher operating temperature than for pure straw (0.075 mass fraction ash). This shows how total ash content is a poor indicator of how problematic a fuel may be during operation in co-combustion. While an increased ash content may warrant considerations such as bed replacement rates or capacity requirements on particulate matter separation systems, it does not inherently cause more ash-related problems.

Interactions between bed particles and bed ash

Figure 3 shows back-scattered electron (BSE) micrographs of the bed material obtained for straw, chicken manure, the high admixture of chicken manure to bark, and the high admixture

of chicken manure to straw. Since heavier elements appear brighter in BSE, K-feldspars are bright bed particles, quartz are darker particles, whereas ash particles typically have a mixed appearance, a homogeneous brightness with void inclusion, or a combination of the two.

As shown in Figure 3 B) and D) there was still a significant impact on the behavior of the fuel ash particles (marked with red circles) in co-combustion of wheat straw with the phosphorus-rich chicken manure at the higher mixture ratio. Wheat straw ash particles formed thin, molten bed ash particles that were enriched in K and Si according to SEM-EDS analysis. However, in co-combustion with large amounts of chicken manure at a significantly higher average bed temperature (Table 3) the bed ash particles formed clusters that interacted to a lesser degree with the bed material. The melting temperature of the formed compounds did cause defluidization, but the tendency to maintain interactions within bed ash particles is similar to that found for chicken manure (Figure 3 A)). Straw and its mixtures with chicken manure therefore defluidized during combustion due to formation of low-temperature melting K-silicates, as expected based on its fuel composition. These observations correspond with a melt induced agglomeration mechanism independent of the used bed material, as it was already proposed for straw [6]. Figure 3 C) shows the bed material after the combustion with bark with high admixtures with chicken manure. No melted bed ash particles could be observed for this case, as well as for pure bark combustion and the low admixture of chicken manure (not depicted in Figure 3).

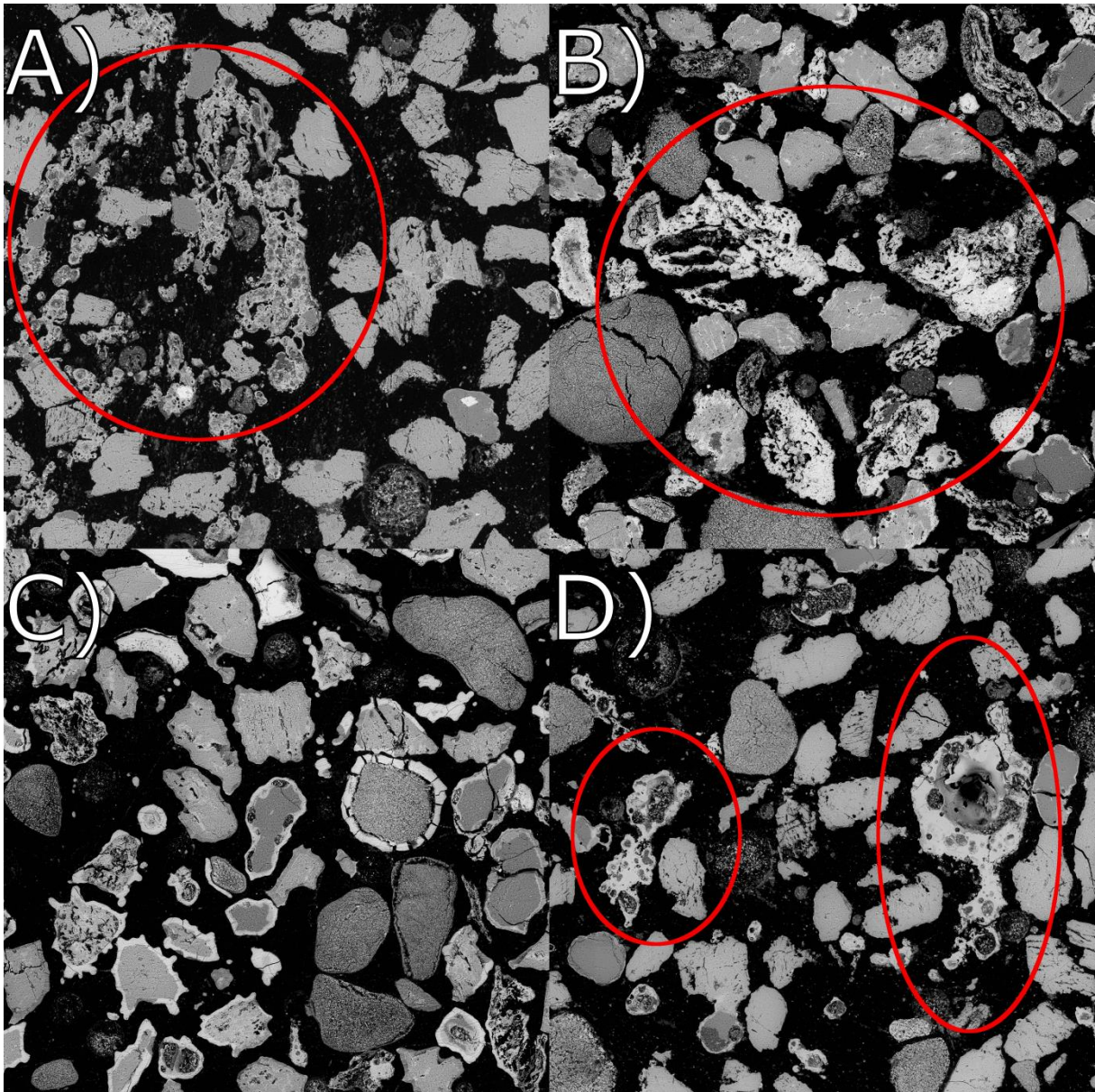


Figure 3. Bed overview images after the combustion of several fuels. Formed ash melt particles are marked with red circles. A) Agglomerate formed in wheat straw combustion, the agglomerate necks consist of silicon, potassium and calcium with hotspots with higher silicon concentrations. B) Bed sample from combustion of chicken manure showing discrete bed particles without agglomerate necks to surrounding bed material. C) No ash melt particles detectable in the bed material after the combustion of bark with high contents of chicken manure. D) Molten bed ash particle agglomerates after the combustion of straw with high admixtures of chicken manure. Limited interaction with bed material is observed, some necks have formed to quartz bed particles.

Morphology of bed particle layers

In this section, the analysis results regarding the morphology of bed particles layers for K-feldspar will be presented in comparison to the better known layer formation on quartz particles. Additionally, typical bed ash particles and/or agglomerates are included in the presentation of the results. Understanding both the ash chemistry related to the agglomeration behavior and the ash layer formation on bed particles gives a more comprehensive insight into the mechanism underlying the inorganic ash chemistry in the fluidized bed reactor, which will be addressed later on. Figure 4 shows BSE micrographs of K-feldspar, quartz, and bed ash particles obtained after combustion.

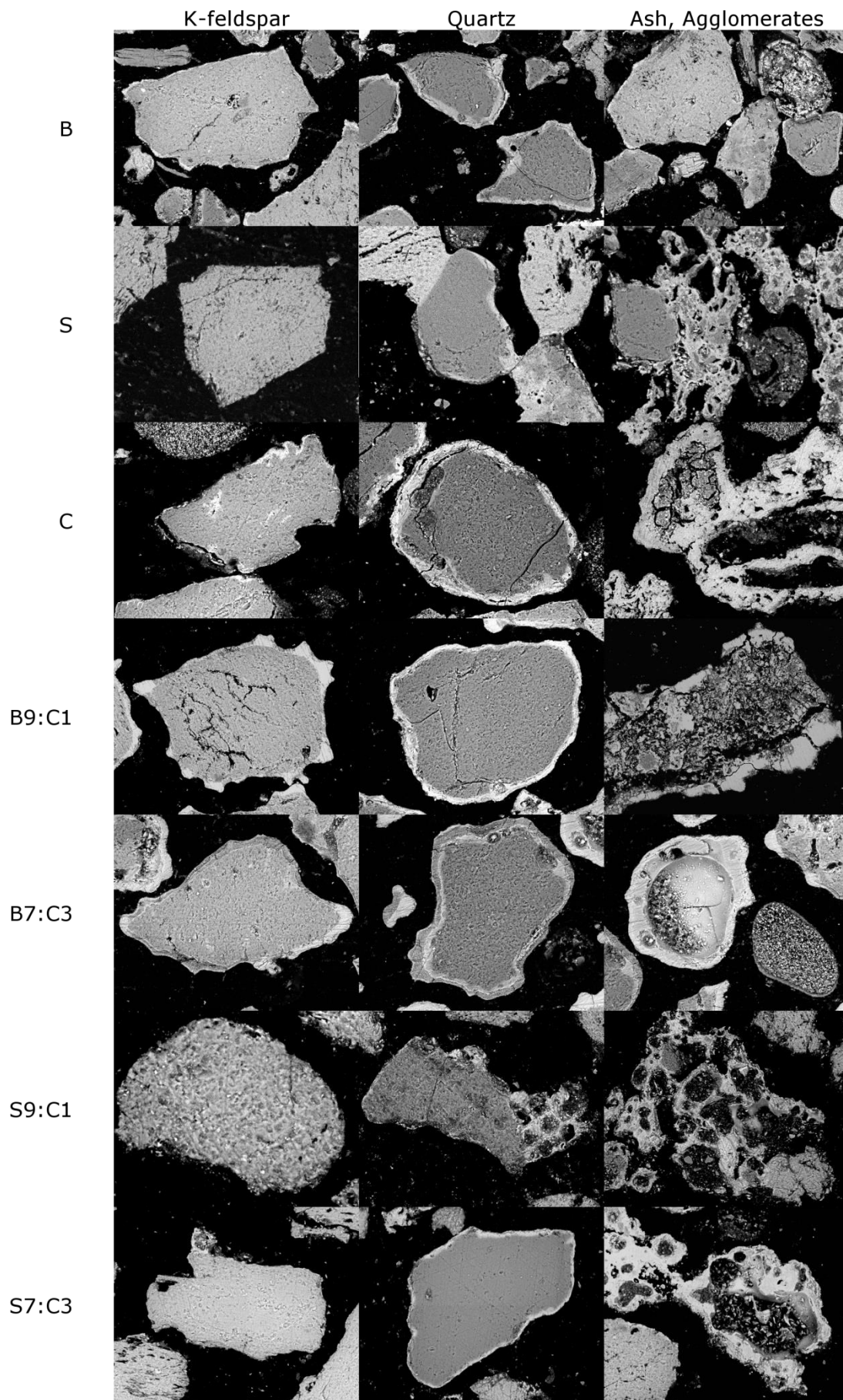


Figure 4. BSE micrographs of the typical bed particles extracted from all experiments. Depicted are K-feldspar, quartz, ash particles and agglomerates.

A continuous outer layer and a thin non-continuous inner layer were observed on K-feldspar bed particles after bark combustion. Similarly, combustion of chicken manure yielded a thin layer on K-feldspar bed particles. Wheat straw did not produce any bed layers on K-feldspar. Considering the extensive presence of molten bed ash particles, this should have been the case if K-feldspar were susceptible to interaction with the K-Si-rich ash from wheat straw. Quartz bed particles display an inner layer formation for all three separate fuels, where a reaction front is observed moving into the quartz bed particle. In the cases of bark and chicken manure, this inner layer on quartz bed particles is covered by an outer layer. For wheat straw, however, this inner layer is mostly interacting with apparently molten bed ash particles by forming necks between particles which likely contributed to the early bed agglomeration.

The fuel mixtures show some interesting differences. Both mixtures of bark and chicken manure produced a thick, non-continuous layer on K-feldspar bed particles. A close-up of a K-feldspar particle can be also seen later on in Figure 7. Considering the large amount of bed ash in the bed after 40 hours, it is likely that at least some of these layers were produced by deposition. This could be further supported by the highly irregular shape of the layers (Figure 4, B7:C3, K-feldspar) which suggests that smaller parts adhered to the layer over time. The low addition of chicken manure to wheat straw showed no layer formation on K-feldspar. Although a thin non-continuous layer was observed on quartz bed particles for this mixture, the amount of agglomerate necks between quartz particle layers and bed ash were reduced compared to the wheat straw case. The high addition level of chicken manure to wheat straw did yield a thin, non-continuous inner layer on quartz bed particles followed by a continuous outer layer. Compared to the low addition of chicken manure to straw, more separate ash melt particles formed in the high addition case. Where interactions with the bed occurred, quartz is highly overrepresented compared to K-feldspar. The occurrence of fewer interactions between ash and bed is likely the reason why the high chicken manure blend with wheat straw could be combusted for a longer time, and at a higher temperature, than what was the case for the other wheat straw cases. The bark and chicken manure mixtures display a similar inner and outer layer on quartz bed particles as for the separate fuels. However, the high chicken manure addition produced an additional set of inner and outer layers. For all the studied cases it was observed that layers formed more readily on quartz bed particles than on K-feldspar, and it seems quartz bed particles with thick inner layers are more prone to participate in agglomerate formation.

Focusing on the ash particles, it becomes obvious that a molten ash fraction can be observed especially for the wheat straw fuel where long, thin streaks of ash have formed instead of breaking up into smaller ash particles. The straw and chicken manure mixtures show bed ash particles that are thicker and more coherent, similar to chicken manure or its high addition to bark. Those ash particles depicted seem to be molten in the inside, while an unmolten outer part is keeping the shape of the particle. Some ash is also present beside the molten regions in seemingly solid state particles. Only in bark are no such homogeneous regions observed.

Composition of bed particle layers

The following discussion will focus on the composition of the particle layers giving further insight into the ash-related interactions with bed particles. The average elemental composition of layers formed on K-feldspar bed particles is shown in Figure 5. Due to lack of layer formations, both wheat straw and its mixture with 10% chicken manure are omitted. It should be noted that in samples with thin layers there is likely data overlap between bed particle composition and layer composition due to the interaction volume of the electron beam. Blends with bark and chicken manure formed outer layers with two different compositions, as seen in Figure 4.

The inner layer composition reveals the initial interaction between ash forming elements in the fuel and K-feldspar bed particles. In an unaffected K-feldspar bed particle (KAlSi_3O_8), the elements K, Al, and Si should be present in the ratio 1:1:3. Elements other than these three, or notably different concentrations through e.g. enrichment of K in relation to Al, indicates which elements in the fuel ash that reacts with the bed particle. The first element that stands out from the rest for all inner layers is calcium. In chicken manure and its mixtures with bark, which were subjected to 40 hours of combustion, magnesium and phosphorus are also detectable as added elements in the inner layer. Considering the overall elemental composition (Figure 1) and the balance of elements in inner layers, it appears as if calcium is present at higher concentrations than would be expected if it was only ash deposition that is responsible for the layer formation. The inclusion of phosphorus and magnesium does suggest that the underlying mechanism could be related to deposition rather than continuous reactions with the bed particle.

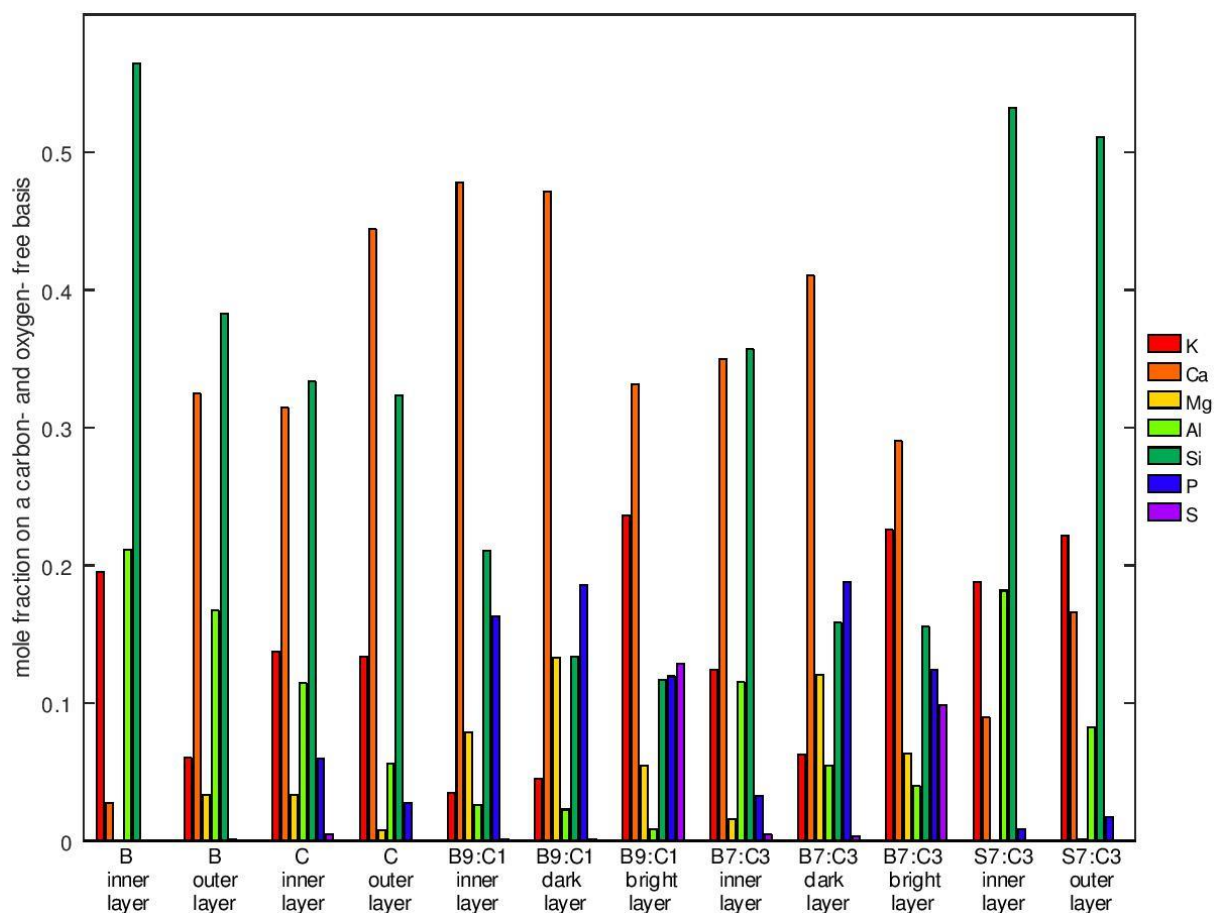


Figure 5. Elemental composition of layers on K-feldspar bed particles as analyzed by SEM-EDS. The nomenclature of “inner” and “outer” describes the location on the particle and not necessarily the underlying mechanism.

The outer layers on K-feldspar also display some interesting features. In the cases with mainly thin layer formation (bark, chicken manure, and its mixture with wheat straw) calcium is still the main deviating element with some traces of magnesium and phosphorus, and more silicon for the straw blend. The thickest layers on K-feldspar were found in co-combustion of bark and chicken manure where there are some other elements present. The brighter layers also contain significant amounts of potassium and sulfur, whereas the darker layers contain magnesium and phosphorus at higher concentrations. This uneven distribution of ash-forming elements suggests a gradual deposition on the bed grain, but it is unclear if the bed particle itself actively participates in the layer build-up or if it is only sticky ash particles.

Interestingly, the ability to retain sulphur in bed ash could prove beneficial from a nutrient recovery point of view as well.

For the analysis of layer formation on quartz bed particles only 2 separate particles were subjected to 3 line scans, since the layer formation on quartz is already described well in literature [4,8,10,13,15]. The elemental analysis (Figure 6) indicates that the layer formation on quartz bed particles follow mechanisms already described in literature. For fuels with little phosphorus available for reaction (bark, straw, and their low mixtures with chicken manure), the quartz bed particle forms an inner layer by reaction with gaseous alkali compounds. This forms a negatively charged silicate matrix that subsequently incorporates calcium if available as is seen for bark in the outer layer. The calcium-rich outer layer may act as a deposition surface for ash particles in the bed, leading to a more varied overall composition. Fuels or mixtures with higher phosphorus content can reduce this interaction by early capture of gaseous alkali compounds, thereby reducing the initial attack on quartz bed particles. This was also observed for the fuel mixtures with chicken manure where the inner layer thicknesses were reduced. Again, a mixed outer layer was observed for bark and high chicken manure where some parts were enriched in potassium and sulphur.

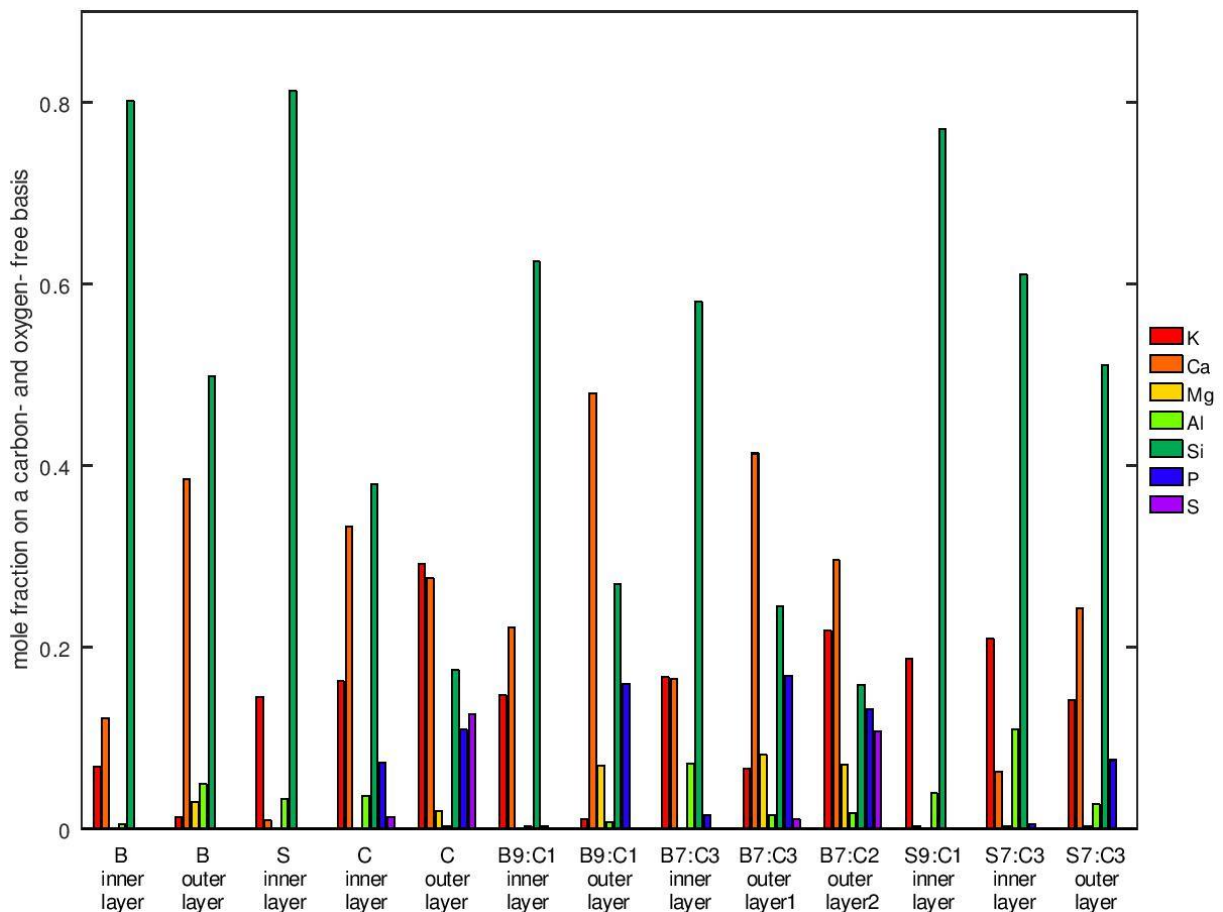


Figure 6. Elemental composition of layers on quartz bed particles as analyzed by SEM-EDS. The nomenclature of “inner” and “outer” describes the location on the particle and not necessarily the underlying mechanism.

Layer formation mechanism for K-feldspar with phosphorus-rich and phosphorus-lean biomass

The layer composition observed in bark combustion and wheat straw with high chicken manure addition showed a migration of calcium into the K-feldspar bed particle layers. In the outer layer a transmigration of potassium out of the particle was observed for bark, and in the co-combustion case it is likely that K-Si-rich ash was deposited outside the inner layer. As

calcium reacted by substitution reactions with the K-feldspar, this could also contribute to an increased K concentration in the outer layer. These observations are in accordance with the mechanism proposed by He et al. [14].

The layer formation of K-feldspars with phosphorus-rich fuels that contained melt formation in bed ash particles seem to follow a different mechanism, since the observed layers are not in accordance with the mechanism proposed by He et al. [14] for woody biomass. High contents of phosphorus seemingly maintain the ash transformation reactions in the bed ash particles rather than promote the substitution of potassium with calcium in K-feldspar. No diffusion of potassium out of the bed particle was observed, leading to the assumption that no or only little direct interaction between K-feldspar and fuel ash occurred. Due to the high reactivity of phosphorus, the formation of calcium, silicon, and potassium phosphates is likely favored as already observed by Grimm et al. for quartz bed particles [4]. This captures these elements into stable compounds, which are not reacting with K-feldspar in the same degree as silicates and oxides. This would lead to the formation of a deposited ash derived outer layer without a distinct reaction or diffusion front into the K-feldspar bed particle, as was commonly found in K-feldspar particles from combustion of chicken manure and its mixtures with bark (Figure 7).

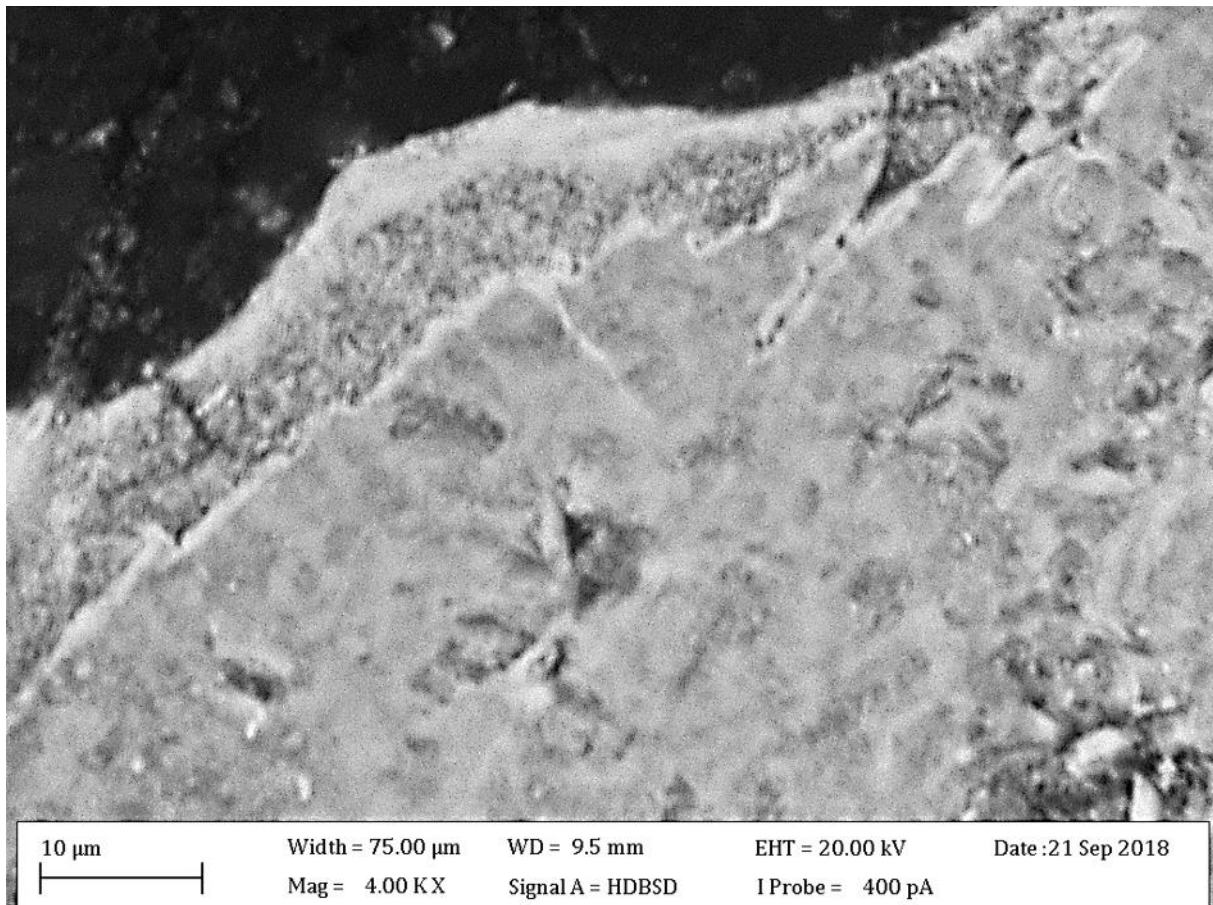


Figure 7. Example of K-feldspar particle with inner and outer layer from co-combustion of bark and chicken manure (B7:C3). The thin inner layer does not show the typical smooth reaction front associated with diffusion-controlled reactions.

Final recommendation on bed material for conversion of phosphorus-rich residues

K-feldspar showed a lower tendency for layer formation compared to quartz and based on layer composition, it is unlikely that layers interacting with K-feldspar would have low

melting temperatures. On the contrary, this would mean that the composition of bed ash particles is more important since the bed material will not act as an alkali capture buffer, as quartz may have some potential to do before an outer, calcium-rich layer is formed. Here it was also concluded that of the bed particles found adhering to molten bed ash, quartz was highly overrepresented for only comprising 4% of the bed material. This is likely caused by the formation of K-silicate inner layers that promote sticking due to low melting temperatures followed by subsequent agglomeration. This may be accentuated by bed ash particles that also contain K-silicates, particularly in the straw cases. K-feldspar may be somewhat protected from such reactions due to the presence of the strong cation Al^{3+} in its structure, whereas quartz does not have any cations that could reduce K^+ inclusion in its SiO_2 structure through strong bonds to the silicate matrix. This could explain the low rate of layer formation in K-feldspar with the exception of inner layers developed through substitution of 2 K^+ with Ca^{2+} .

If the melting temperature of bed ash particles could be controlled through fuel composition, K-feldspar could very well be a highly suitable bed material even in co-combustion with phosphorus-lean fuels such as wheat straw. The resistance to reactions with gaseous alkali compounds is an important property to avoid layer formation and subsequent shedding of potentially sticky bed particle layers. The application of phosphorus-rich fuels as a way to decrease the agglomeration tendency of difficult fuels proved successful. By shifting the ash chemistry to the formation of phosphates the ash melting point of the ash in the fluidized bed was increased. Further understanding the chemistry underlying ash – bed material interactions makes it possible to better predict the behavior of a certain fuel and bed material combination. Fuel design is a method using this approach. Focusing on the ash of available fuels it would be possible to mix them in such a way that agglomeration is minimized [32].

From a nutrient recovery point of view, this could open up for more phosphorus-rich residues to be included in the fuel. Although some of the nutrient-rich ash may be sticking to bed material, the clear dissociation of fuel ash particles and bed particles of both kinds at high phosphorus fuel content would suggest that it could be separated. Further research should be focused on the bioavailability of phosphorus and possible other nutrients found in the bottom ash as individual bed particles and in the bed particle layers. If the phosphorus in the layers has sufficient bioavailability, fertilization directly with used bed material might be thinkable, especially if a harmless natural mineral like K-feldspar is being used.

Conclusion

K-feldspar will mainly interact with fuel ash through substitution of potassium in K-feldspar with calcium, a reaction that was largely mitigated with phosphorus-rich fuel. Instead, it seemed as if phosphorus-rich ash particles deposited as an outer layer, with little or no direct interaction with the bed particle itself. The interaction between bed material and fuel ash is therefore an important factor influencing bed fluidization. The ash composition, especially the phosphorus content, plays an important role in layer formation mechanisms. Co-combusting bark with phosphorus-rich chicken manure changed the underlying mechanisms regarding bed material – ash interactions and shifted the interactions from the bed material surface into the ash phase by reducing the amount of calcium available for the reaction with the bed material.

Adding phosphorus-rich chicken manure to wheat straw as fuel in fluidized bed combustion reduced the bed agglomeration tendency by increasing the melting temperature of the produced ash. While it was not possible to observe layers on K-feldspar with pure straw as fuel, the admixture of enough chicken manure led to a long enough operational time for layers to form. These results highlight that the fuel ash content is not a good indicator for ash

related problems and that an understanding of the underlying ash chemistry is more important to be able to handle different fuels.

This work also highlighted the usability of K-feldspar as alternative bed material. Its reduced interaction with the fuel ash compared to quartz makes it less susceptible for interactions with bed ash. If fully understood the reduced interactions might make it possible to use challenging fuels in a K-feldspar bed.

Acknowledgments

This study was carried out within the Bioenergy2020+ GmbH projects N200560 and C200410. Bioenergy2020+ GmbH is funded within the Austrian COMET program, which is managed by the Austrian Research Promotion Agency (FFG) and promoted by the federal government of Austria as well as the federal states of Burgenland, Niederösterreich, and Steiermark. We are grateful for the support of our project partner, the Institute of Chemical Engineering at the TU Wien. Furthermore, we would like to thank the Swedish national strategic research program Bio4Energy (Thermochemical platform and Environmental and nutrient recycling platform). Additionally, the Kempe Foundation is thanked for their financial support of the post-doc research of Matthias Kuba at Umeå University and Luleå University of Technology. The authors acknowledge the facilities and technical assistance from Cheng Choo Lee of the Umeå Core Facility for Electron Microscopy (UCEM - NMI node) at the Chemical Biological Centre (KBC), Umeå University.

References

- [1] Lang B. Marktanalyse Energieholz. Wien: Österreichische Energieagentur - Austrian Energy Agency; 2014.
- [2] Stagg R, Ward S. Timber Price Indices. For Res 15:05:06.929681+00:00. <https://www.forestresearch.gov.uk/tools-and-resources/statistics/statistics-by-topic/timber-statistics/timber-price-indices/> (accessed July 16, 2018).
- [3] Kuba M, He H, Kirnbauer F, Boström D, Öhman M, Hofbauer H. Deposit build-up and ash behavior in dual fluid bed steam gasification of logging residues in an industrial power plant. *Fuel Process Technol* 2015;139:33–41. doi:10.1016/j.fuproc.2015.08.017.
- [4] Grimm A, Skoglund N, Boström D, Öhman M. Bed Agglomeration Characteristics in Fluidized Quartz Bed Combustion of Phosphorus-Rich Biomass Fuels. *Energy Fuels* 2011;25:937–47. doi:10.1021/ef101451e.
- [5] Kunii D, Levenspiel O. *Fluidization engineering*. 2. ed. Boston: Butterworth-Heinemann; 1991.
- [6] De Geyter S, Öhman M, Boström D, Eriksson M, Nordin A. Effects of Non-Quartz Minerals in Natural Bed Sand on Agglomeration Characteristics during Fluidized Bed Combustion of Biomass Fuels. *Energy Fuels* 2007;21:2663–8. doi:10.1021/ef070162h.
- [7] Öhman M, Pommer L, Nordin A. Bed Agglomeration Characteristics and Mechanisms during Gasification and Combustion of Biomass Fuels. *Energy Fuels* 2005;19:1742–8. doi:10.1021/ef040093w.

- [8] Brus E, Öhman M, Nordin A. Mechanisms of Bed Agglomeration during Fluidized-Bed Combustion of Biomass Fuels. *Energy Fuels* 2005;19:825–32. doi:10.1021/ef0400868.
- [9] Tranvik AC, Öhman M, Sanati M. Bed Material Deposition in Cyclones of Wood Fuel Fired Circulating Fluidized Beds (CFBs). *Energy Fuels* 2007;21:104–9. doi:10.1021/ef060175f.
- [10] He H, Ji X, Boström D, Backman R, Öhman M. Mechanism of Quartz Bed Particle Layer Formation in Fluidized Bed Combustion of Wood-Derived Fuels. *Energy Fuels* 2016;30:2227–32. doi:10.1021/acs.energyfuels.5b02891.
- [11] Kirnbauer F, Hofbauer H. The mechanism of bed material coating in dual fluidized bed biomass steam gasification plants and its impact on plant optimization. *Powder Technol* 2013;245:94–104. doi:10.1016/j.powtec.2013.04.022.
- [12] Kuba M, He H, Kirnbauer F, Skoglund N, Boström D, Öhman M, et al. Thermal Stability of Bed Particle Layers on Naturally Occurring Minerals from Dual Fluid Bed Gasification of Woody Biomass. *Energy Fuels* 2016;30:8277–85. doi:10.1021/acs.energyfuels.6b01523.
- [13] He H, Boström D, Öhman M. Time Dependence of Bed Particle Layer Formation in Fluidized Quartz Bed Combustion of Wood-Derived Fuels. *Energy Fuels* 2014;28:3841–8. doi:10.1021/ef500386k.
- [14] He H, Skoglund N, Öhman M. Time-Dependent Layer Formation on K-Feldspar Bed Particles during Fluidized Bed Combustion of Woody Fuels. *Energy Fuels* 2017. doi:10.1021/acs.energyfuels.7b02386.
- [15] He H, Skoglund N, Öhman M. Time-Dependent Crack Layer Formation in Quartz Bed Particles during Fluidized Bed Combustion of Woody Biomass. *Energy Fuels* 2017;31:1672–7. doi:10.1021/acs.energyfuels.6b02980.
- [16] He Z, Lane DJ, Saw WL, van Eyk PJ, Nathan GJ, Ashman PJ. Ash–Bed Material Interaction during the Combustion and Steam Gasification of Australian Agricultural Residues. *Energy Fuels* 2018;32:4278–90. doi:10.1021/acs.energyfuels.7b03129.
- [17] Zhou C, Rosén C, Engvall K. Biomass oxygen/steam gasification in a pressurized bubbling fluidized bed: Agglomeration behavior. *Appl Energy* 2016;172:230–50. doi:10.1016/j.apenergy.2016.03.106.
- [18] Vuthaluru HB, Zhang DK. Remediation of ash problems in fluidised-bed combustors. *Fuel* 2001;80:583–98. doi:10.1016/S0016-2361(00)00116-2.
- [19] Vuthaluru HB, Zhang D. Effect of Ca- and Mg-bearing minerals on particle agglomeration defluidisation during fluidised-bed combustion of a South Australian lignite. *Fuel Process Technol* 2001;69:13–27. doi:10.1016/S0378-3820(00)00129-6.
- [20] Wagner K, Kuba M, Häggström G, Skoglund N, Öhman M, Hofbauer H. Influence of Phosphorus on the Layer Formation on K-feldspar During Fluidized Bed Combustion and Gasification. *Eur Biomass Conf Exhib Proc* 2018;26th EUBCE-Copenhagen 2018:486–92. doi:10.5071/26thEUBCE2018-2BO.6.2.
- [21] Berguerand N, Berdugo Vilches T. Alkali-Feldspar as a Catalyst for Biomass Gasification in a 2-MW Indirect Gasifier. *Energy Fuels* 2017;31:1583–92. doi:10.1021/acs.energyfuels.6b02312.

- [22] Wagner K, Mauerhofer AM, Kuba M, Hofbauer H. Suitability of K-feldspar as Alternative Bed Material in Dual Fluidized Bed Steam Gasification in Combination with Ash-Rich Feedstocks. 23rd Int. Conf. FBC, Seoul, Korea: 2018, p. 967–76.
- [23] Boström D, Skoglund N, Grimm A, Boman C, Öhman M, Broström M, et al. Ash Transformation Chemistry during Combustion of Biomass. *Energy Fuels* 2012;26:85–93. doi:10.1021/ef201205b.
- [24] Rockström J, Steffen W, Noone K, Persson Å, Chapin FS, Lambin EF, et al. A safe operating space for humanity. *Nature* 2009;461:472–5. doi:10.1038/461472a.
- [25] Adam C, Peplinski B, Michaelis M, Kley G, Simon F-G. Thermochemical treatment of sewage sludge ashes for phosphorus recovery. *Waste Manag* 2009;29:1122–8. doi:10.1016/j.wasman.2008.09.011.
- [26] Cordell D, Rosemarin A, Schröder JJ, Smit AL. Towards global phosphorus security: A systems framework for phosphorus recovery and reuse options. *Chemosphere* 2011;84:747–58. doi:10.1016/j.chemosphere.2011.02.032.
- [27] Ashley K, Cordell D, Mavinic D. A brief history of phosphorus: From the philosopher's stone to nutrient recovery and reuse. *Chemosphere* 2011;84:737–46. doi:10.1016/j.chemosphere.2011.03.001.
- [28] Koppatz S, Pfeifer C, Hofbauer H. Comparison of the performance behaviour of silica sand and olivine in a dual fluidised bed reactor system for steam gasification of biomass at pilot plant scale. *Chem Eng J* 2011;175:468–83. doi:10.1016/j.cej.2011.09.071.
- [29] Stoffdaten | Product data; Feldspat FS 900 S | Feldspar FS 900 S n.d.
- [30] Öhman M, Nordin A. A New Method for Quantification of Fluidized Bed Agglomeration Tendencies: A Sensitivity Analysis. *Energy Fuels* 1998;12:90–4. doi:10.1021/ef970049z.
- [31] Ester M, Kriegel H-P, Sander J, Xu X, others. A density-based algorithm for discovering clusters in large spatial databases with noise. *Kdd*, vol. 96, 1996, p. 226–231.
- [32] Skoglund N. Ash chemistry and fuel design focusing on combustion of phosphorus-rich biomass. Doctoral Thesis. Department of applied physics and electronics, Umeå universitet, 2014.

Supplementary

Table S. 1. Fuel fingerprint data; concentrations given in mol kg⁻¹.

	B	S	C	B9:C1	B7:C3	S9:C1	S7:C3
K	0.04	0.24	0.36	0.07	0.14	0.30	0.36
Na	0.06	0.02	0.36	0.09	0.13	0.04	0.09
Ca	0.15	0.09	1.18	0.39	0.65	0.25	0.61
Mg	0.07	0.03	0.65	0.16	0.26	0.07	0.15
Fe	0.07	0.01	0.03	0.07	0.06	0.02	0.02
Al	0.26	0.04	0.08	0.17	0.17	0.04	0.06
Si	0.53	0.79	0.24	0.48	0.47	0.72	0.68
P	0.03	0.02	1.14	0.15	0.35	0.08	0.24
S	0.03	0.04	0.24	0.04	0.07	0.05	0.07
Cl	0.01	0.01	0.29	0.02	0.07	0.01	0.02